Turbulence and Microstability Considerations for AT Operation

Bill Dorland, Institute for Plasma Research, University of Maryland at College Park

March 11, 1999

Turbulence and Transport Modeling

- Develop and run turbulence codes
- Try to gain broad insights
- Build simplified transport models from simulation results
- Test models against experimental data

New physics impacts every phase.

ETG Modes

- Consider the following very simple model of ETG modes. Taking $k_\parallel = 0$, and ignoring the difference between curvature and ∇B drifts, the electrostatic electron density evolution equation simplifies to

$$\frac{\partial n}{\partial t} + \nabla \cdot \left(n \mathbf{v}_E + \frac{2p}{m\Omega B^2} \mathbf{B} \times \nabla \mathbf{B} \right) = 0$$

- Linearizing and Fourier transforming this equation, one finds

$$-i\omega n - i\omega_* \Phi + 2i\omega_d \Phi - 2i\omega_d p = 0$$

- Similarly, the linearized pressure evolution equation is

$$-i\omega p - i\omega_* (1 + \eta_e)\Phi + 3i\omega_d \Phi - i\omega_d \left(6p - 3n\right) = 0.$$

- Defining $\tau \equiv T_e/T_i$ and $b \equiv (k_\perp \rho_e)^2$, quasineutrality yields:

$$\Phi = -\frac{n}{\tau + b}$$

These equations may be combined to yield a quadratic dispersion relation:

$$(\tau + b)\omega^2 + \left[6\omega_d(\tau + b) - \omega_* + 2\omega_d\right]\omega$$

$$+6\omega_d^2(1 + \tau + b) + 2\omega_*\omega_d(\eta_e - 2) = 0$$

ETG Modes

- One may solve for ω to find

$$\omega = -\frac{B}{2A} \pm \frac{\sqrt{B^2 - 4AC}}{2A}$$

where

$$A = \tau + b$$

$$B = 6\omega_d(\tau + b) - \omega_* + 2\omega_d,$$

$$C = 6\omega_d^2(1 + \tau + b) + 2\omega_*\omega_d(\eta_e - 2)$$

- Consider the flat density limit. Then, this expression simplifies to

$$\omega = -\frac{3\omega_d(\tau + b) + \omega_d}{\tau + b} \pm \frac{\sqrt{3\omega_d^2(\tau + b)^2 + \omega_d^2 - 2\omega_d\omega_*\eta_e(\tau + b)}}{\tau + b}$$

- Instability requires ω_d and ω_* have the same sign. This occurs on the outboard midplane, and is what is meant by "bad curvature."

- Note that large $\tau = T_e/T_i$ is stabilizing for ETG modes. This may correspond to "hot electron modes," such as observed on TORE-SUPRA.

Transport from ETG Modes

- So far, the linear theory of ETG modes look a lot like ITG modes, except that the normalizing quantities are very different. In fact, the diffusion expected from ETG modes naturally scales like

$$\chi_e \sim \frac{\rho_e^2 v_{te}}{L_{ne}} \ll \frac{\rho_i^2 v_{ti}}{L_{ne}}$$

- Thus, if ETG and ITG modes co-existed and were fully analogous, and $\chi_i \sim 1$ m^2/sec, then the expected value of $\chi_e \sim 0.02$ m^2/sec. This would be experimentally irrelevant.

- Even if χ_i were as large as simulations suggest and therefore large enough to enforce marginal stability, it turns out that the expected value of χ_e would be too small to be relevant to experiments.

- However, simulations provide more insight than this. Non-saturating streamers observed, with $\chi_e \geq 40$ m^2/sec for typical parameters. This is certainly large enough to enforce electron temperature profile consistency, and to be an important limiting factor in internal transport barriers.

- Next step is to include missing physics, especially magnetic perturbations.

Shear-flow Generation in ITG Modes

- Consider ITG modes. In a hydrogenic plasma, quasineutrality guarantees that the electron and ion densities are equal. Ignoring trapped electrons, induction and collisions, the electron response is determined from Ohm's law:

$$\nabla_{\|}(p_e - |e|\Phi) = 0.$$

- Thus, the electron density is given by

$$n_e = \frac{|e|}{T}\left(\Phi - \langle\langle \Phi \rangle\rangle\right).$$

- Note that $\langle\langle n_e \rangle\rangle = 0$ (or at most a constant) in this limit. This is the appropriate result for adiabatic electrons.

- Considering now guiding center ion quantities, quasineutrality dictates

$$\frac{|e|}{T}\left(\Phi - \langle\langle \Phi \rangle\rangle\right) = n_i + \frac{\nabla_\perp^2}{2}\left(n_i + T_{\perp i} + 2\Phi\right)$$

- Taking the flux surface average of this equation, and substituting results from the density and temperature evolution equations yields:

$$\frac{\partial E_r'}{\partial t} = -\langle\langle \mathbf{v}_E \cdot \nabla n_i \rangle\rangle - \left\langle\left\langle \nabla_\perp^2 \mathbf{v}_E \cdot \nabla p_{\perp i} \right\rangle\right\rangle$$

- That is, a sheared radial electric field is driven by the nonlinear flux of ion guiding centers and ion pressure.

Shear-flow Generation in ETG Modes

- The story is quite different for ETG modes.
- At modest values of $k_\perp \rho_e$, where ETG modes tend to be, $k_\perp \rho_i$ is very large. The ion response is therefore adiabatic. Mathematically, the ion density response is well approximated by

$$n_i^{tot} = \Gamma_0^{1/2} \left(n_i + \frac{\hat{\nabla}_\perp^2}{2} T_{\perp i} \right) + (\Gamma_0 - 1) \frac{q\Phi}{T}$$

- For large b, $\Gamma_0(b) \propto b^{-1/2}$, and $\hat{\nabla}_\perp^2(b) \sim -1/2$. Thus, the gyrophase independent part of the ion density is small. Only the last part of the last term survives,

$$n_i^{tot} \sim -\frac{q\Phi}{T}$$

- Thus, for ETG modes, there is no obvious strong drive of E_r' from particle and heat fluxes.

$$\bar{n}_e + (1 - \Gamma_0)\, \Phi = -\tau\Phi$$

$$E_r' = \langle\langle \tau\Phi + \bar{n}_e \rangle\rangle$$

- So, we turn to simulations to find out what happens. The result is striking!

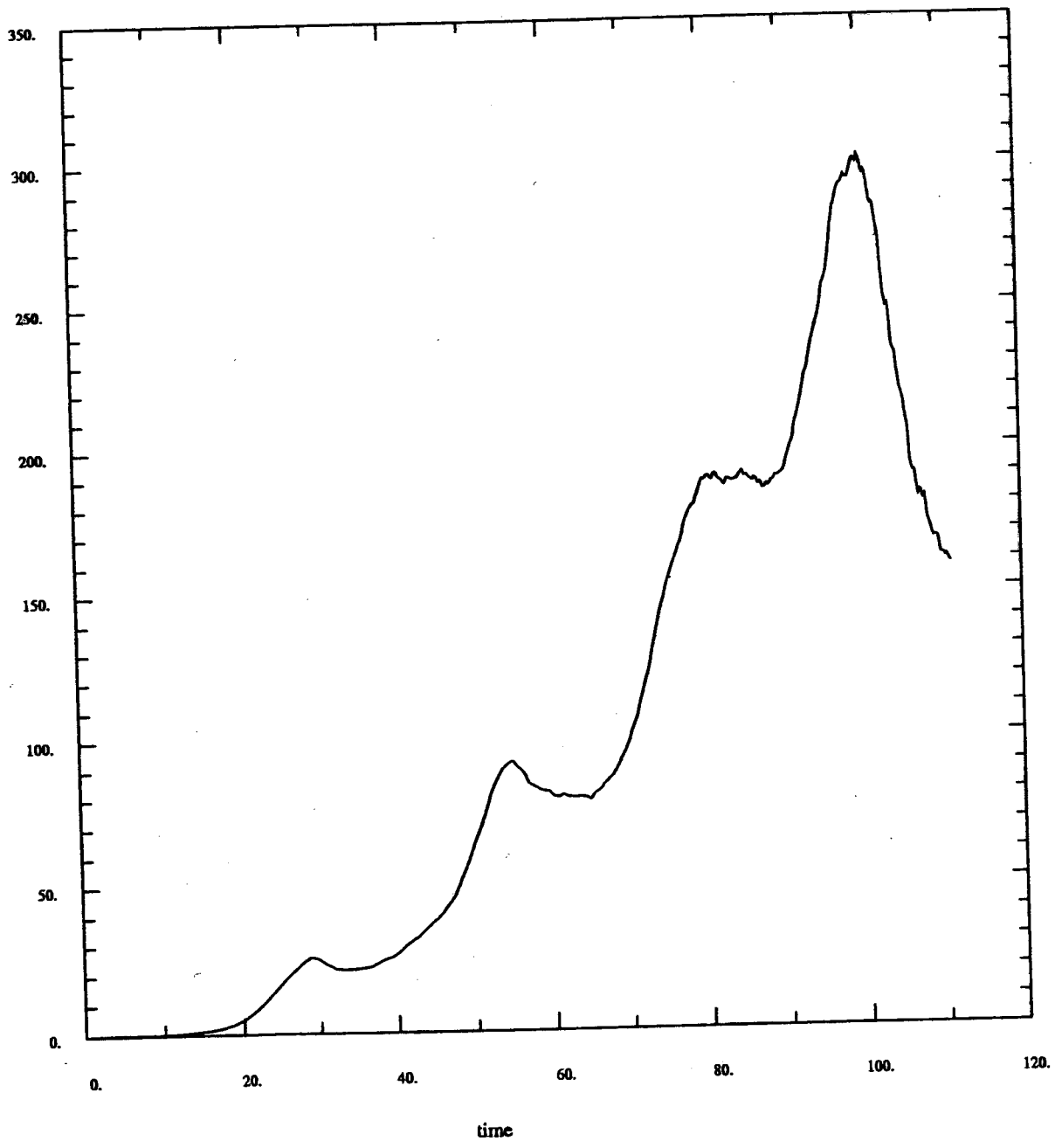
Thermal Flux
350.
300.
250.
200.
150.
100.
50.
0.
0.
20.
40.
60.
80.
100.
120.
time

Potential

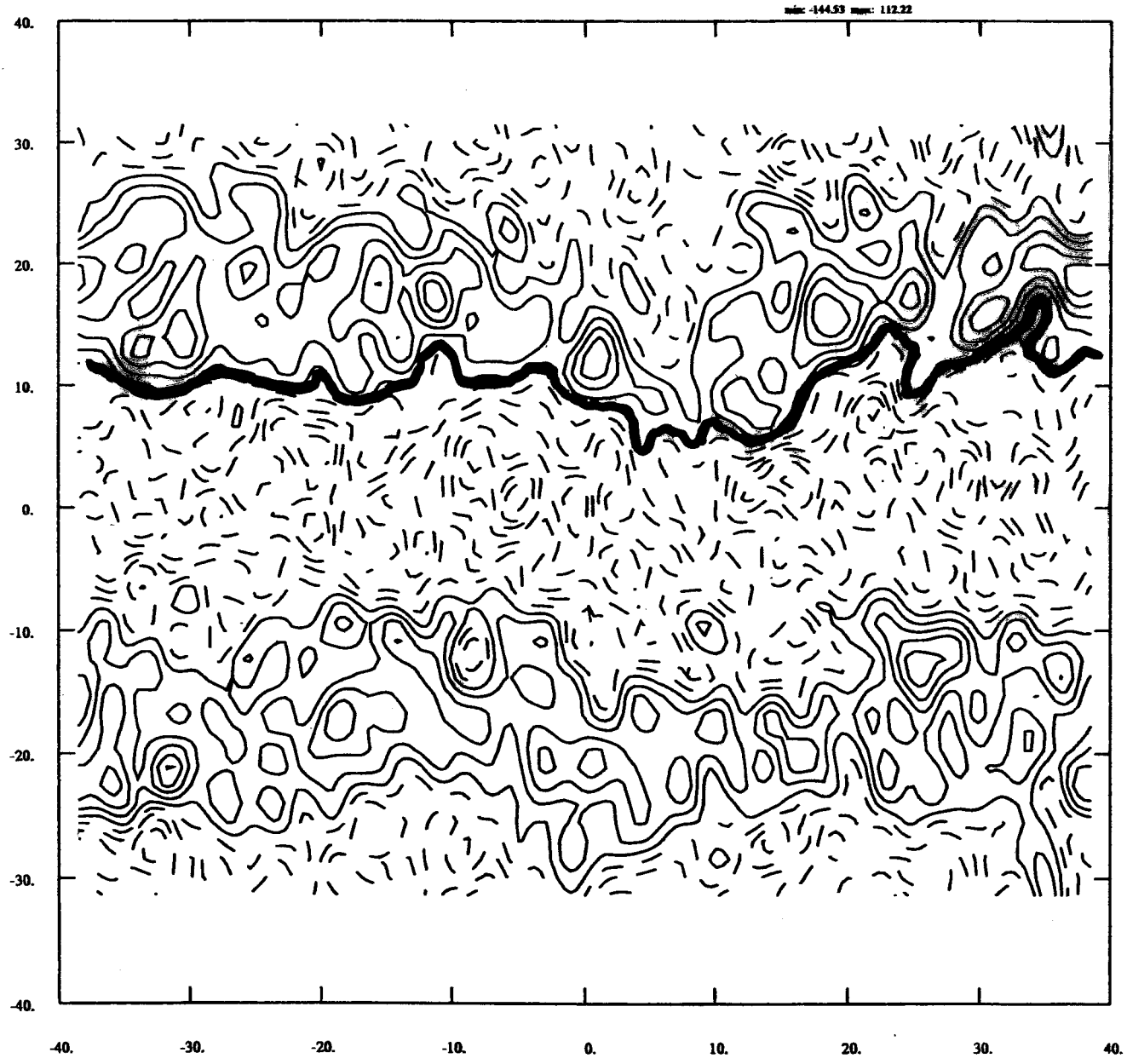
min: -144.53 max: 112.22
40.
30.
20.
10.
0.
-10.
-20.
-30.
-40.
-40.
-30.
-20.
-10.
0.
10.
20.
30.
40.

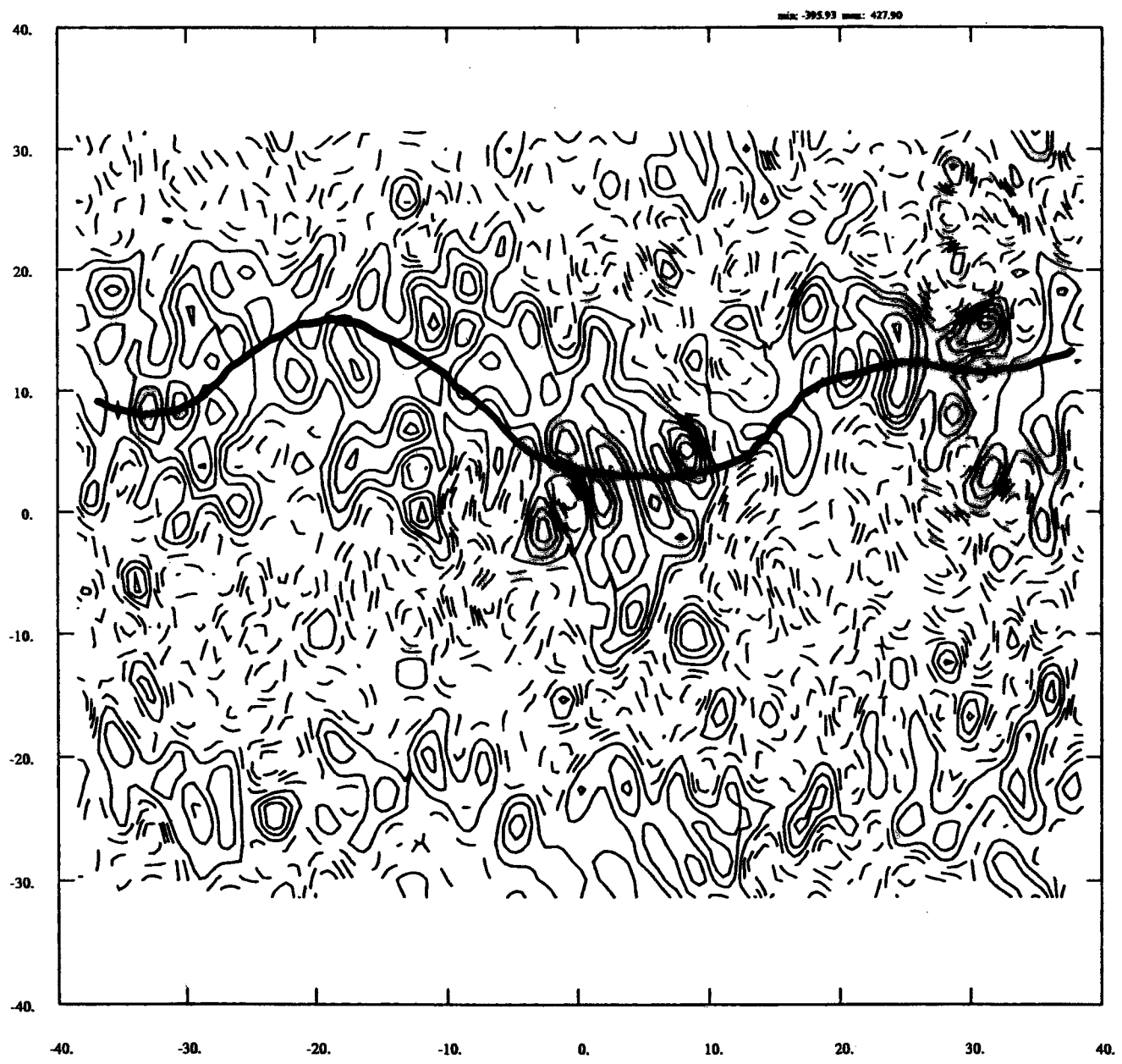
Perp Temp
min: -395.93 max: 427.90
40.
30.
20.
10.
0.
-10.
-20.
-30.
-40.
-40.
-30.
-20.
-10.
0.
10.
20.
30.
40.

AT Physics Codes

- GS2 is a linear, parallel, electromagnetic, gyrokinetic, multiple species, general geometry code. Almost certainly describes linear physics.
- Available online (send email to bdorland@ipr.umd.edu)
- MDS+ interface to data coming from MIT
- Runs on workstation in multiiples of a couple of minutes; runs on parallel machine in a few seconds.
- Easily embedded in larger code. Someone should make a GK version of GLF23.

Experimental Comparisons

- Models improving over time.
- Transient transport experiments: response is fast enough, but qualitative only
- ECH perturbation experiments: ion channel better than the electron channel
- Waltz, *et al.*, improved interpolation scheme from IFS-PPPL. GLF23 model should work for wider range of parameters.
- Ernst has incorporated flow shear into IFS-PPPL, finds improved agreement for TFTR Supershots.
- Future: greater reliance on GK simulations (linearly and nonlinearly).

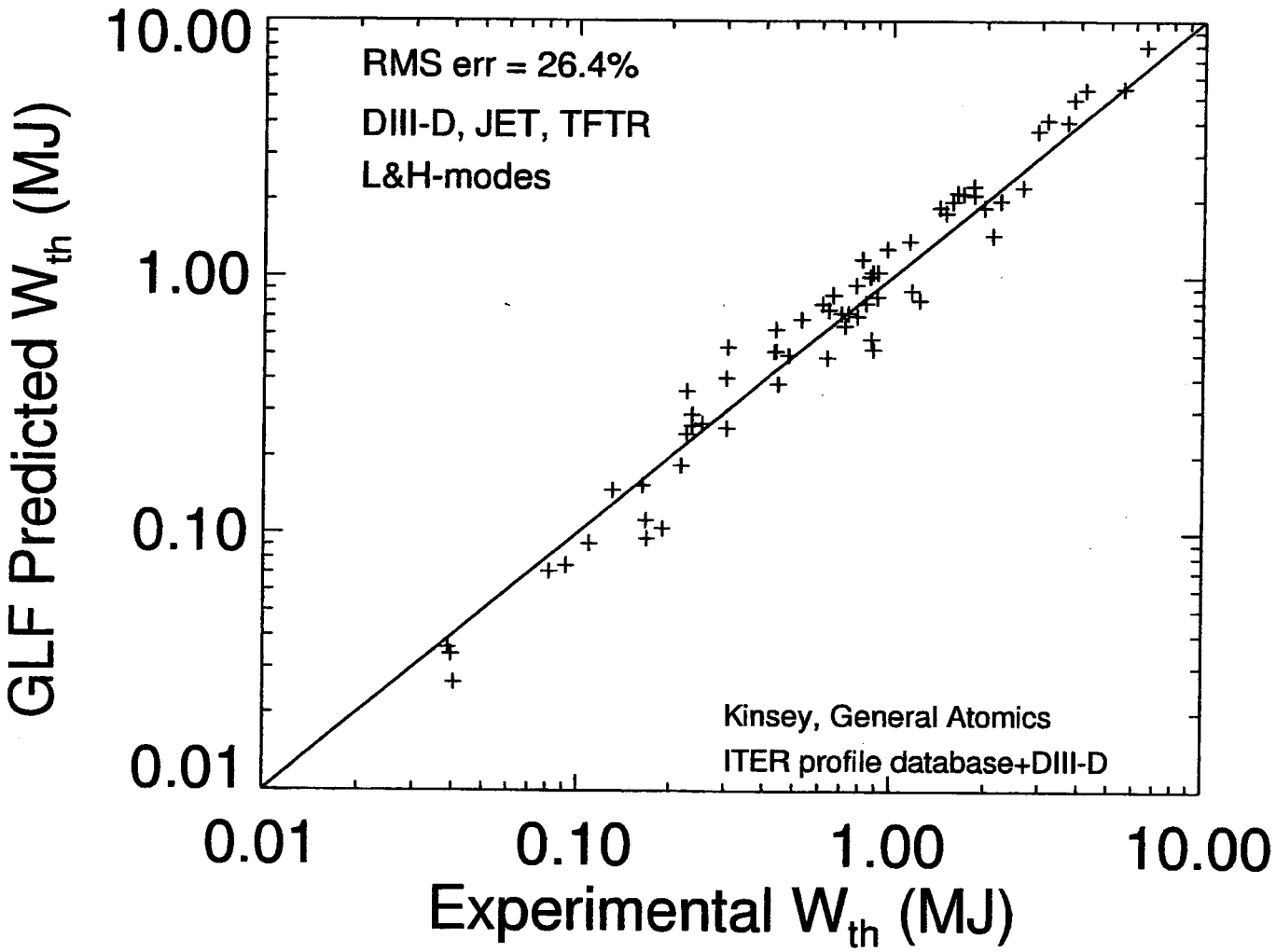
RMS err = 26.4%
DIII-D, JET, TFTR
L&H-modes
Kinsey, General Atomics
ITER profile database+DIII-D
GLF Predicted W_{th} (MJ)
Experimental W_{th} (MJ)
10.00
1.00
0.10
0.01
0.01
0.10
1.00
10.00

Gyrokinetic Equation

- The toroidal gyrokinetic equation is structurally plain:

$$\frac{df}{dt} = \bar{C}_\ell f$$

- The linearized collision operator is used here. In the collisionless limit, the conservation of the distribution function at it evolves in phase space is evident.

- More explicitly,

$$\frac{d}{dt} = \frac{\partial}{\partial t} + \dot{\mathbf{X}} \cdot \nabla + \dot{U} \frac{\partial}{\partial U},$$

$$\dot{\mathbf{X}} = U \left(\hat{\mathbf{b}} + \langle \delta \mathbf{B}_\perp \rangle \right) + \frac{\hat{\mathbf{b}}}{m\Omega} \times \left(\mu \Omega \nabla \ln B + m U^2 \hat{\mathbf{b}} \cdot \nabla \hat{\mathbf{b}} \right)$$

$$+ \frac{c\hat{\mathbf{b}}}{B} \times \nabla \left(\langle \delta \Phi \rangle - \left\langle \delta \mathbf{A}_\perp \cdot \frac{\mathbf{v}_\perp}{c} \right\rangle \right)$$

$$\dot{U} = -\frac{q}{mc} \frac{\partial \langle \delta A_\parallel \rangle}{\partial t} - \frac{q}{m} \left(\hat{\mathbf{b}} + \frac{\langle \delta \mathbf{B}_\perp \rangle}{B} \right) \cdot \nabla \langle \delta \Phi \rangle$$

$$- \frac{1}{m} \left(\hat{\mathbf{b}} + \frac{\langle \delta \mathbf{B}_\perp \rangle}{B} \right) \cdot \nabla \left(\mu \Omega - q \left\langle \delta \mathbf{A}_\perp \cdot \frac{\mathbf{v}_\perp}{c} \right\rangle \right)$$

$$- \frac{cU\hat{\mathbf{b}}}{B} \times \left(\hat{\mathbf{b}} \cdot \nabla \hat{\mathbf{b}} \right) \cdot \nabla \left(\langle \delta \Phi \rangle - \left\langle \delta \mathbf{A}_\perp \cdot \frac{\mathbf{v}_\perp}{c} \right\rangle \right)$$

Gyrokinetic Maxwell's Equations

- Poisson's equation expresses quasineutrality:

$$\sum_s q_s n_s = 0$$

  and determines $\delta\Phi$ implicitly.

- Ampere's law is separable into parallel and perpendicular components:

$$\nabla_\perp^2 \delta A_\parallel = -\frac{4\pi}{c} \sum_s q_s \int d^3v \, v_\parallel F_{1s}$$

$$\nabla_\perp \delta B_\parallel \times \hat{\mathbf{b}} = \frac{4\pi}{c} \sum_s q_s \int d^3v \, v_\perp F_{1s}$$

- In these expressions, the distribution functions and the densities include the gyrophase dependent and independent components. For this reason, the polarization drift appears as a term in the quasineutrality constraint.

Gyrokinetic Description of Plasma

- The distribution function depends on spatial and velocity coordinates:

$$f_s = f_s(x, y, z, E, \lambda, \mathrm{sign}(v_\parallel))$$

- Discretization is expensive. For example, for each species,

$2n_x n_y n_z n_E n_\lambda = 2{\cdot}64{\cdot}32{\cdot}96{\cdot}10{\cdot}40 \sim 157,000,000$ points

- Compare with high-end fluid turbulence simulations:

$$n_x n_y n_z = 512^3 \sim 134,000,000 \text{ points}$$

- Gyrokinetic problem is highly anisotropic in phase space. Non-uniform meshes used for the along-the-field-line, energy and pitch angle coordinates.
- Parallel pseudo-spectral algorithm used to evaluate nonlinear terms on spatially twisted field-line-following coordinate grid.
- Fast time scales associated with electron and Alfvén dynamics in problem require implicit time advancement scheme for linear terms.
- Size of problem forces one to use large parallel computers with multiple domain decomposition techniques. Parallelism implemented using MPI and SHMEM libraries.
- Parallel computers not available five years ago; gyrofluid model developed to enable progress.

E_r shear becomes more important as T_i increases

- 1994 IFS-PPPL model reproduces balanced deuterium NBI L-Modes
- At higher temperatures in supershots, the 1994 IFS-PPPl model falls short of reaching measured temperatures by up to 50%

~ Balanced D0 L-Mode

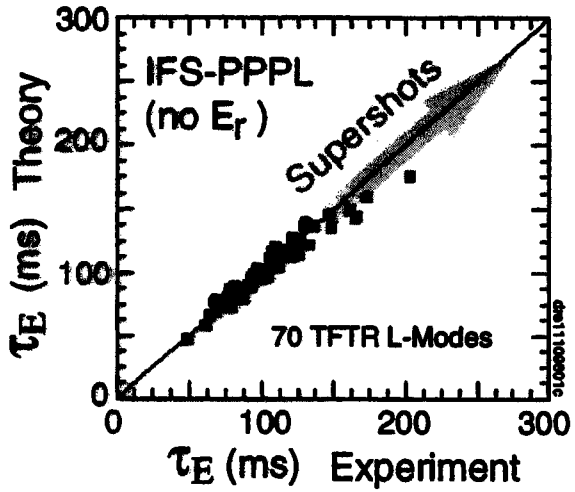

Kotschenreuther, Dorland, Beer, Hammett, Phys. Plasmas (1995)

~ Balanced D0 & T0 Supershots

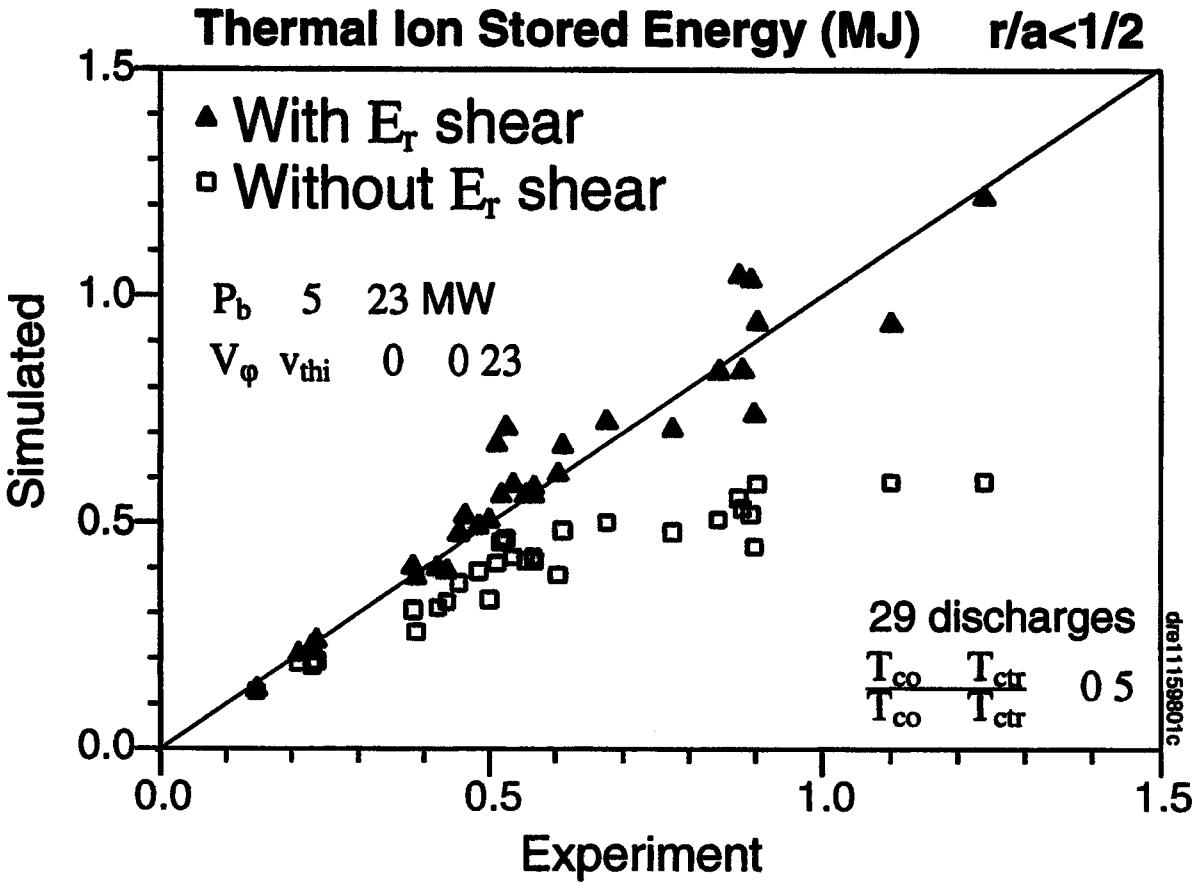

- *Including Er, using new scaling for V_θ, reproduces supershots*

Ernst, et al., Phys. Rev. Lett., Sept. (1998) & IAEA (1998)

PPPL PRINCETON PLASMA

IFS-PPPL Model on C-MOD

- Schachter, *et al.*, carefully tested IFS-PPPL model against four shots from C-MOD: 2L, 2H
- Model fits T_i profile of one H-mode, otherwise fails. Error appears to be in critical gradient (model tends to underpredict R/L_T).
- C-MOD collisionality higher than allowed by parameterization.
- GS2 installed at C-MOD with MDS+ interface to data. Should allow direct calculations of linear critical gradients, *etc.*
- Ross, *et al.*, doing large number of nonlinear simulations directly for the experimental parameters, including trapped electrons, impurities, general geometry. Finds sensitivity to impurity density gradient is important. (TTF) Also testing frequency and wavenumber spectra against measurements.

Rosenbluth-Hinton Effect

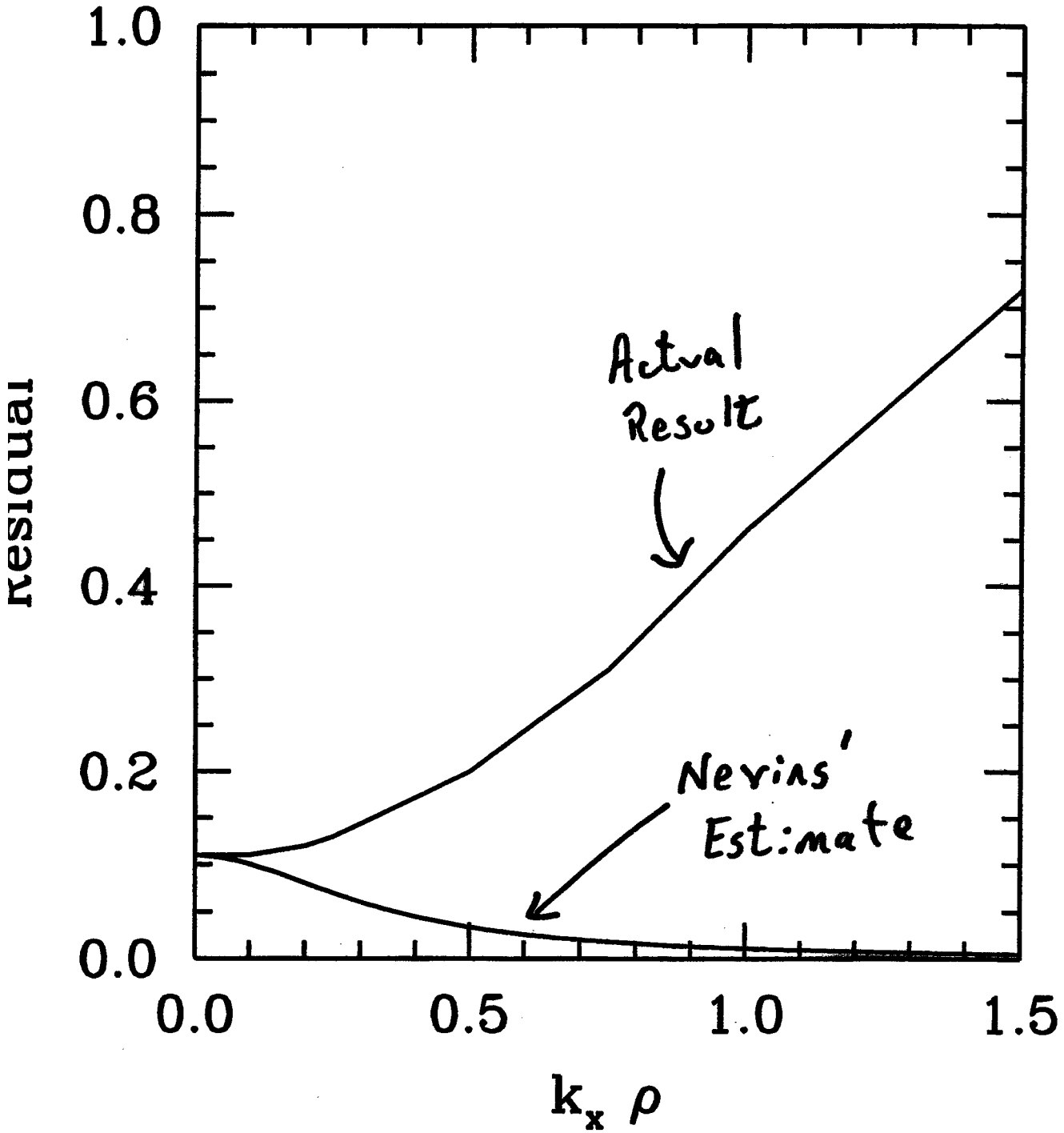

Residual increases with k_ρ.

RH Depends on Geometry

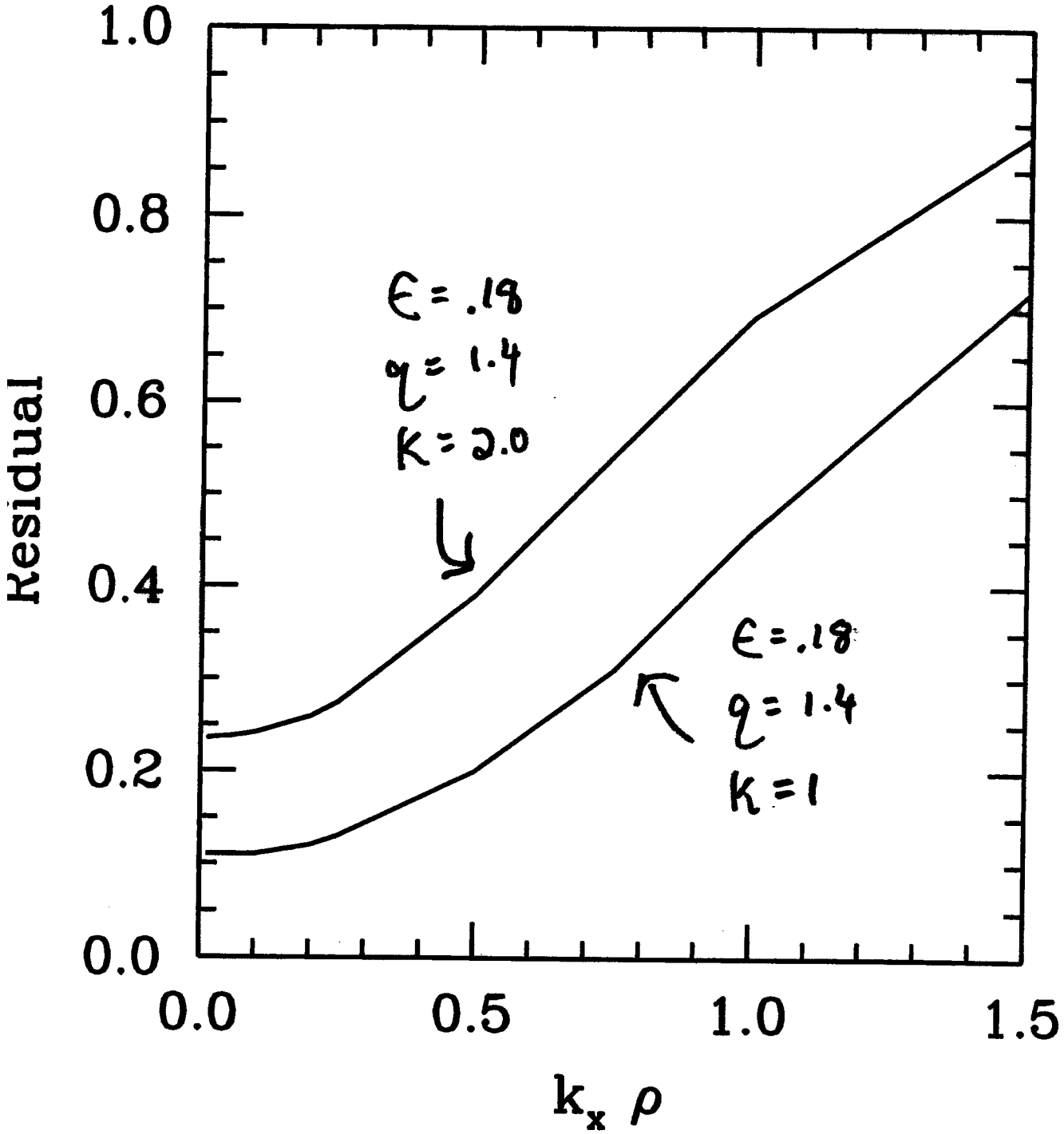

Physics Improvements

- Rosenbluth-Hinton (RH) effect still being studied.
- Electromagnetic, multi-species, collisional effects potentially important; mitigate RH effect.
- Shaping enhances RH effect
- Nonlinear extension of GS2 running now. Fully gyrokinetic and electromagnetic flux tube simulations possible on big computers.
- Ultimately, particle noise is problem because of RH
- Electron transport needs more attention.

Rogers & Drake Pedestal Simulations

Pedestal exceeds ideal limit

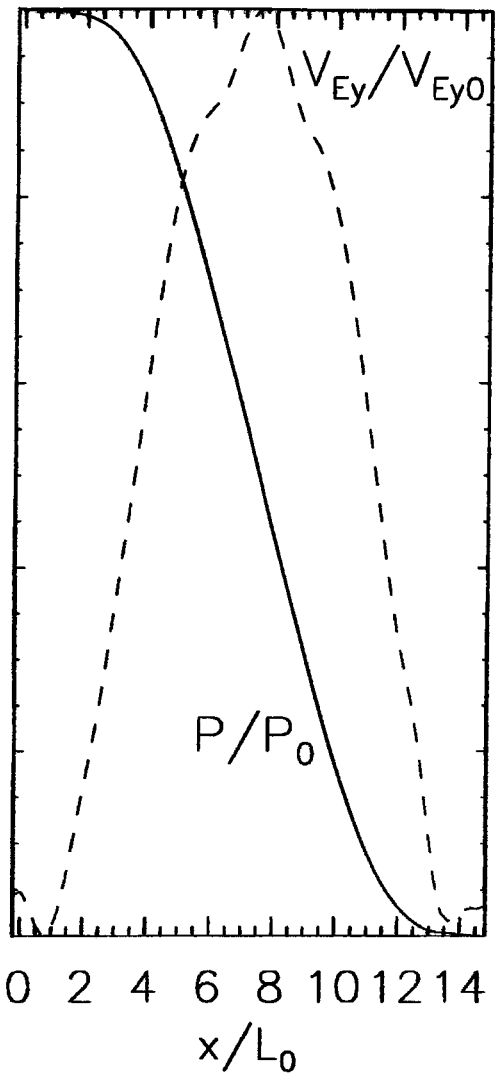

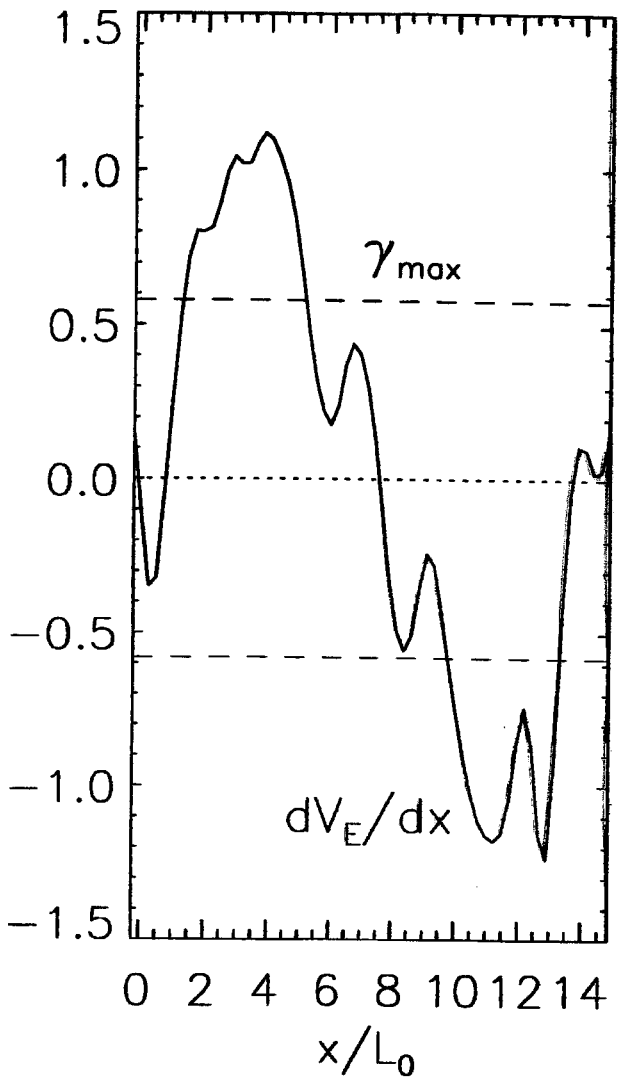

- **Max(α)=1.8α_{crit} but no ideal modes**
- **In center $V'_{E\times B} \simeq 0$, so $V'_{E\times B}$ not enough**
  - ▷ **Stability is due to ω_{*i}**

ω_{*i} can stabilize all modes because gradient is radially localized

---

- **Essential physics in simple ramp gradient model:**

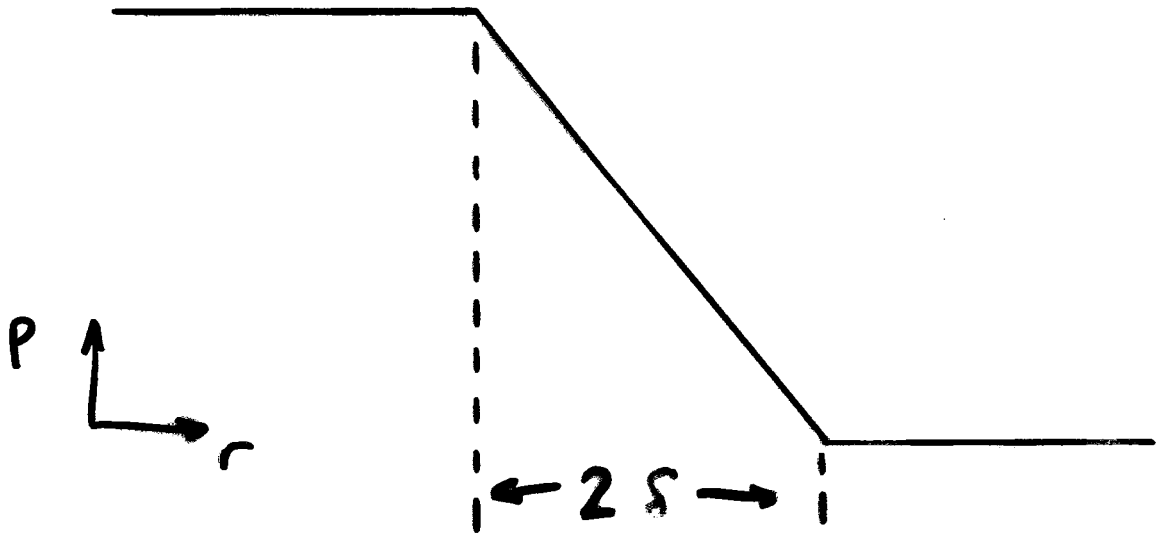

- **Dispersion relation:** $\omega(\omega+\omega_{*i}) = -\gamma_0^2$ **with**

$$\gamma_0^2 \simeq \left(\left[\frac{|k_\theta\delta|}{|k_\theta\delta|+1}\right]\alpha - 1\right)\frac{V_A^2}{q^2R^2}$$

- **Modes with** $k_\theta\delta \ll 1$ **always stable** $(\alpha \sim 1)$

- **Modes with higher** $k_\theta\delta$ **stable if** $\omega_{*i} > 2\gamma_0$.

Modified Ideal Stability Boundary

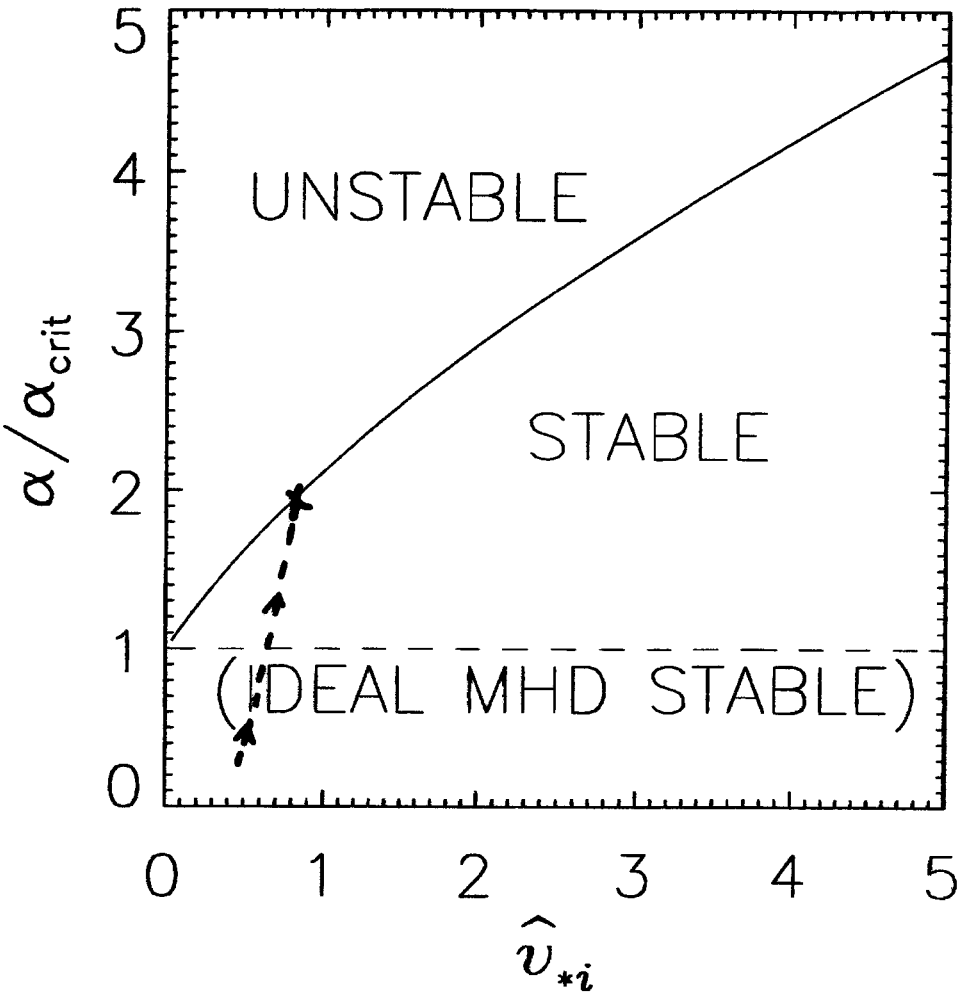

- $\hat{v}_{*i} = V_{*i} t_0/\delta = \frac{\rho_i}{\delta}\left(\frac{T_i}{T_i+T_e}\frac{R}{2\delta}\right)^{1/2}$

- **Explains why pedestal exceeds ideal MHD boundary**
  - **in simulations**
  - **in experiments ?**

Edge Pressure Gradient May Exceed Infinite n Ballooning Limit Due to Small Barrier Width

- Theory of Rogers, Drake and Zeiler predicts p' may exceed infinite n ballooning limit due effect of the small extent of the steep gradient region on long wavelength modes, and diamagnetic effect at short wavelength

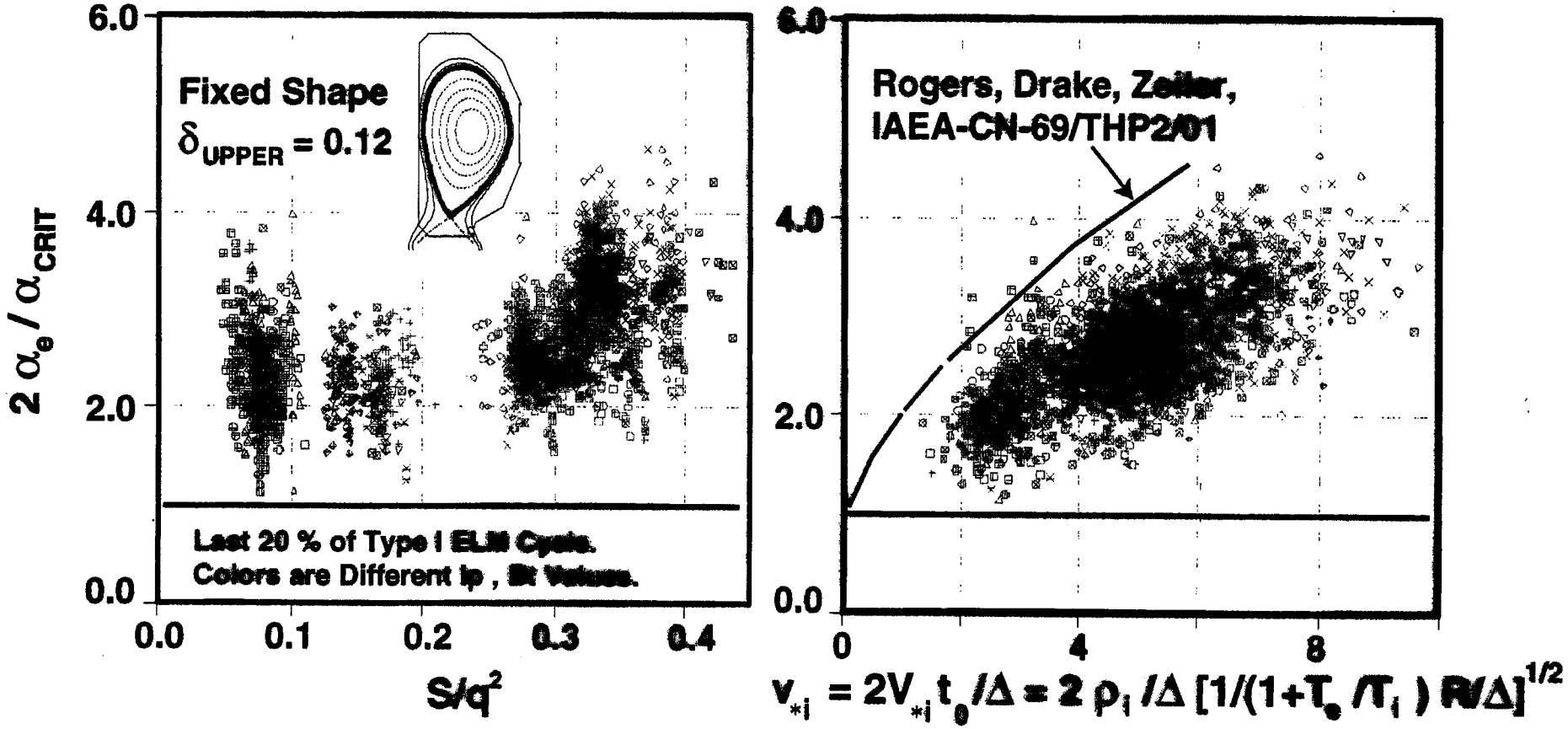

T. Osborne

Performance of Barrier

- β_{Ped} independent of pedestal width in high $\hat{\nu}_{*i}$ limit.

$$\beta_{Ped} \propto \frac{\alpha_{crit}}{q^2}\left(\frac{\rho_i}{R}\right)^{2/3}$$

- But, wide pedestal not understood.

Important Aspects of Barriers

- High T_i/T_e
- thermal ion dilution
- Z_{eff}
- weak $\hat{s}$
- high α_{MHD}
- Strong shaping
- high $\omega'_{E\times B}$
- strong heating/torque/ fuelling inside ρ

Conclusions

- ETG modes can provide relevant level of electron thermal transport
- Physics codes for AT transport/turbulence, μ-stability becoming available
- RH effect stronger at high k_r, strong shaping
- Barrier simulations of Rogers & Drake are being compared against data. Predict performance of barrier can be independent of barrier width (for narrow barriers)